OBSERVATION

If one carefully considers the act of observing the dimple in the mechanical model, something appears to be wrong. It must be remembered that free ripples in the sheet play the role of light in the analogy. To observe the model with the electromagnetic light of the laboratory is analogous to observing the real electrodynamic universe with a phantasmic radiation vastly exceeding the speed of light.

ACKNOWLEDGMENT

The author gratefully acknowledges the assistance and counsel of Wayne T. Picciano in the preparation of this paper.

A Laboratory Linear Analog for Lattice Dynamics*

R. B. RUNK, J. L. STULL, AND O. L. ANDERSON
Alfred University, Alfred, New York
(Received 19 June 1963)

The application of the linear air track, a laboratory demonstration apparatus, is extended to demonstrate theorems in lattice dynamics. As a one-dimensional model it, visually and quantitatively, reveals details of the frequency versus wavenumber diagram, in particular the various modes of vibration, dispersion, phase velocity, the separation between the acoustic and optic branches, and the frequency spectrum.

I. INTRODUCTION

LATTICE dynamics is a recognized discipline lying mostly in the province of mathematical physics. Consequently, it is difficult to teach its important concepts to the uninitiated. The purpose of this paper is to describe a laboratory model which allows the important theorems in lattice dynamics to be visualized by the student. Townsend[1] has recently announced one such model which produces frequencies in the low audio range. The present model differs in that it demonstrates frequencies in the 1-cps range.

II. APPARATUS

The linear air track[2,3] is a modification of a similar apparatus reported by Neher and Leighton.[4] It consists [Fig. 1(a)] of a 2-×2-in. hollow square aluminum extrusion, oriented with a diagonal vertical and connected by adjustment screws to an I-beam or other rigid support. Air at a pressure of about 1 psi is forced through four rows of 0.0225-in.-diam holes in the track. This pressure supports "cars" of various designs, made from standard 2-×2-in.-extruded aluminum angle. The retardation of a car due to the viscosity of the air cushion is such that the characteristic time (the time required for the velocity to decay to $1/e$ of its initial value) is about 200 sec. This is the chief advantage of the apparatus in that it allows observation of dynamic phenomena without the interference of friction.

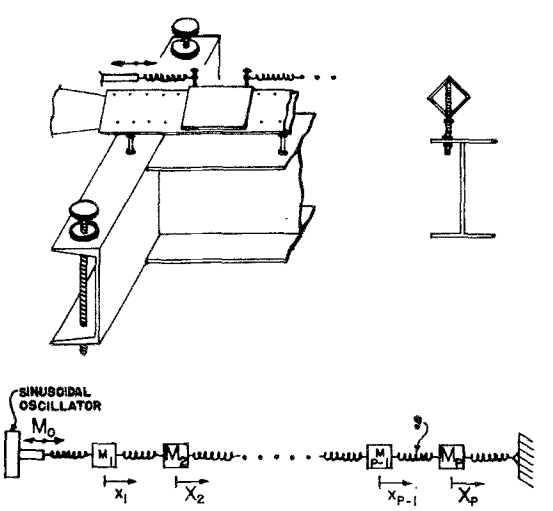

FIG. 1. (a) Linear air track; (b) diatomic linear chain at equilibrium.

* This work supported in part by the College Center of the Finger Lakes.
[1] J. R. Townsend, Am. J. Phys. **31**, 470 (1963).
[2] John L. Stull, Am. J. Phys. **30**, 839 (1962).
[3] John L. Stull, Bull. Am. Phys. Soc. **8**, 444 (1963).
[4] H. V. Neher and R. B. Leighton, Am. J. Phys. **31**, 255 (1963).

The lattice dynamical analog to be described has been constructed to study the normal modes of vibration of a linear chain of free particles interconnected by springs. The chain comprises p cars of adjustable mass, supported on a 21-ft track, and $(p+1)$ identical coil springs. One of the two end springs of the chain is anchored rigidly to the track and the other attached to a variable speed mechanical oscillator. The modes of vibration of the chain are found by slowly sweeping the oscillator frequency. When a resonance appears, the oscillator is switched off to prevent excessive vibration and to establish the desired fixed end. The frequency can be measured with some precision since the vibration persists for several minutes. The phase velocity in the chain can be measured directly by imposing a sinusodial pulse at one end of the chain and timing its arrival at the other end.

If the masses of the cars in the chain alternate between two values, one has an analog for a one-dimensional diatomic ionic crystal, such as NaCl. A simpler monatomic analog can also be produced by making the masses of all cars the same. These analogs differ from the real crystal, of course, due to the fixed ends, but the use of suitable boundary conditions takes this into account. Such analogs reveal visual and quantitative details of the frequency versus mode number (wavenumber) diagram, in particular the various modes of vibration, dispersion, phase velocity, the separation between acoustic and optic branches, the stopping band and its relation to mass ratio, and the frequency spectrum.

The behavior of a finite diatomic chain with fixed ends can be treated following the method of Born and von Karman[5] for an infinite chain and using the method of Rayleigh[6] to impose end conditions. The chain is represented in Fig. 1(b), in which $\frac{1}{2}p$ particles of mass m alternate with $\frac{1}{2}p$ particles of mass $M>m$, each connecting spring having a spring constant κ.

The displacements of particles M_j and m_j from their equilibrium positions is given by X_j and x_j, the subscript denoting the position of the particle in the chain. The chain is bounded by the fixed ends of the track. However, as an aid in inserting the boundary conditions, the chain is considered to be bounded by two stationary particles M_0 and m_{p+1}. The equations of motion for M_j and m_{j+1} are

$$\begin{aligned} Md^2X_j/dt^2-\kappa(x_{j+1}+x_{j-1}-2X_j)&=0\\ md^2x_{j+1}/dt^2-\kappa(X_{j+2}+X_j-2x_{j+1})&=0. \end{aligned} \tag{1}$$

Solutions are sought for which the displacements of particles vary sinusoidally, both with time and with the positions of particles in the chain. Thus,

$$\begin{aligned} X_j&=Ae^{ij\alpha}\sin(\omega t+\phi),\\ x_{j+1}&=ae^{i(j+1)\alpha}\sin(\omega t+\phi), \end{aligned} \tag{2}$$

where a and A are the amplitude constants. Since Eq. (2) must satisfy the boundary conditions, $X_0=x_{p+1}=0$, α is as follows:

$$\alpha=N\pi/(p+1), \tag{3}$$

where N is an integer.

Substitution of the values of X_j and x_{j+1} into (1) yields two solutions for ω^2,

$$\begin{aligned} \omega^2&=(2\kappa/M)[1-(a/A)\cos\alpha]\\ &=(2\kappa/m)[1-(A/a)\cos\alpha], \end{aligned} \tag{4}$$

from which

$$A=\frac{a\{(M-m)\pm[(M+m)^2-4Mm\sin^2\alpha]^{\frac{1}{2}}\}}{2M\cos\alpha}. \tag{5}$$

Therefore, Eq. (4) may be written

$$\begin{aligned} \omega^2=(\kappa/Mm)\{&M+m\\ &\mp[(M+m)^2-4Mm\sin^2(N\pi/p+1)]^{\frac{1}{2}}\}. \end{aligned} \tag{6}$$

Thus, for the general diatomic case the frequency versus wavenumber curve has two branches separated by a gap. When $m/M\rightarrow 0$, this gap becomes large, the frequency for the upper branch approaches

$$\omega=(2\kappa/m)^{\frac{1}{2}}, \tag{7a}$$

and the frequency for the lower branch approaches

$$\omega=(2\kappa/M)^{\frac{1}{2}}\sin[N\pi/(p+1)]. \tag{7b}$$

On the other hand, when $M=m$, Eq. (6) reduces to the equation for the monatomic case,

$$\omega=(4\kappa/m)^{\frac{1}{2}}\sin[N\pi/2(p+1)]. \tag{8}$$

[5] M. Born and Th. von Karman, Physik. Z. **13**, 297 (1912); see also, Max Born and Kun Huang, *Dynamical Theory of Crystal Lattices* (Clarendon Press, Oxford, England, 1954).

[6] Lord Rayleigh, *The Theory of Sound* (Dover Publication, Inc., New York, 1945) (Reprint), Vol. I, p. 174.

III. THE LINEAR MONATOMIC MODEL

Equation (8) expresses angular frequency, $\omega = 2\pi\nu$, as a function of mode number. Frequency may also be expressed in terms of wavenumber $k = 1/\lambda$. Since $N = 2L/\lambda = 2kL$ and $L = (p+1)r$, where L is the length of the chain and r is the equilibrium interparticle distance, Eq. (8) for the monatomic chain may also be written

$$\omega = (4\kappa/m)^{\frac{1}{2}} \sin\pi kr \tag{9}$$

or

$$\nu = kr(\kappa/m)^{\frac{1}{2}}(\sin\pi kr/\pi kr). \tag{10}$$

These are the expressions more common in lattice dynamics.[7] The ν vs k curve for the infinite monatomic chain is continuous, the frequency varying from zero at $k = 0$, $\lambda = \infty$, to a maximum, $\omega_A = (4\kappa/m)^{\frac{1}{2}}$, at $k_m = 1/(2r)$. The ν vs k curves for the finite chains are identical with that for the infinite chain possessing the same lattice constants, m, κ, and r, except that they are discontinuous, the extreme values approaching the above limits as the number of particles increases.

Dispersion (the nonlinearity between frequency and wavenumber) becomes observable only for large values of wavenumber where the wavelength approaches the order of magnitude of the interparticle distance. In cases where λ is much larger than the interparticle spacing, $k \to 0$ and Eq. (9) becomes analogous to the familiar equation for a longitudinal elastic standing wave in a solid,

$$\omega = (N\pi/L)(E/\rho)^{\frac{1}{2}},$$

where E is the elastic modulus and ρ is the density.

In a monatomic solid where $r \approx 10^{-8}$ cm, frequencies of the order of 10^{12} cps are required before dispersion is observed. In such a solid, essentially all waves with frequencies between zero and ν_A are allowed to propagate, but any wave with a frequency above ν_A is reflected. Thus, the solid is a low pass filter.

In the linear-air-track model of the monatomic chain, described above, the lattice constants used were $\kappa = 5040$ dyn/cm, $m = 155.6$ g, and $r = 34$ cm. Therefore, dispersion became apparent at frequencies less than 1 cps. Because of the low resonant frequencies of the system, each mode of vibration can be observed in detail, from the first, where all the members move in phase, to the last, where every member moves exactly out of phase with its nearest neighbors. The six observed modes of vibration for a six-member chain are shown schematically in Fig. 2. This figure illustrates the direction and amplitude of each chain member and the effects due to the end conditions.

Figure 3 shows the ν vs k diagram for a linear chain with the above constants. The solid line

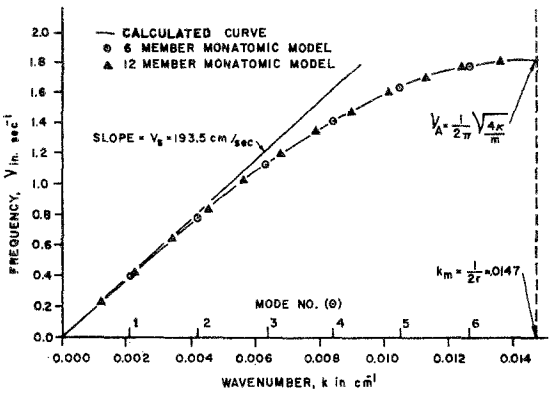

FIG. 3. The ν vs k diagram for a monatomic chain. The solid line represents the calculated curve for the infinite chain and the points indicate the measured values for the 6- and 12- member chains.

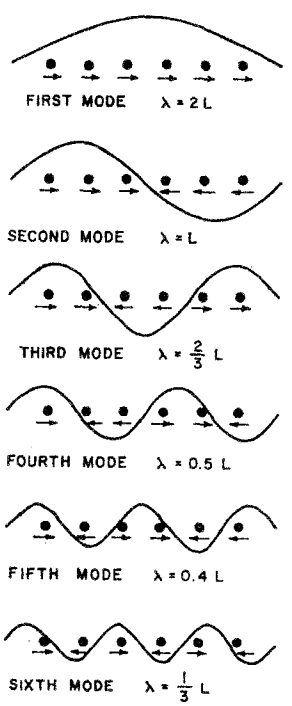

FIG. 2. Amplitude variation curves for the 6-member monatomic chain.

[7] Leon Brillouin, *Wave Propagation in Periodic Structures* (Dover Publications, Inc., New York, 1953) (Reprint).

TABLE I. Comparison of frequencies calculated from Eq. (9) and those experimentally measured for a 6-member monatomic model with the chain constants, $\kappa = 5040$ dyn/cm, $m = 155.6$, and $r = 34$ cm.

Mode number	Wavenumber cm^{-1}	Calculated frequency cps	Measured frequency cps
1	2.1×10^{-3}	0.404	0.407
2	4.2	0.786	0.788
3	6.3	1.130	1.130
4	8.4	1.417	1.410
5	10.5	1.633	1.630
6	12.6	1.767	1.770

is a plot of Eq. (9) for an infinite number of particles. The points show the measured values for a six- and a twelve-particle system. The quantitative agreement between the frequencies measured and the frequencies calculated from Eq. (9) is shown in Table I.

Many important physical constants may be derived from the frequency versus wavenumber diagram. For instance, from the diagram in Fig. 2, the velocity of an elastic wave along the chain (analogous to the velocity of sound in a solid) may be obtained. This velocity is equal to the slope of the curve as $k \rightarrow 0$. From Eq. (10),

$$\lim_{\kappa \to 0} \frac{\nu}{k} = r\left(\frac{\kappa}{m}\right)^{\frac{1}{2}} = \left(\frac{r\kappa}{m/r}\right)^{\frac{1}{2}} = V_s,$$

where $r\kappa$ is the elastic modulus of the chain and m/r is its density.

This velocity was determined for the above monatomic models from the measured values of the constants r, κ, and m; from the experimental slope in Fig. 2; and from the measurement of the rate at which a low-frequency sinusoidal pulse was propagated along the chain. The three determinations yielded velocities of 193.5, 192.0, and 190 cm/sec, respectively.

IV. THE LINEAR DIATOMIC MODEL

A one-dimensional diatomic ionic crystal can be represented by alternating two different masses evenly spaced along a chain. The introduction of this second mass effectively doubles the number of degrees of freedom of the system which leads to the degeneracy of the frequency with wavenumber, shown in Eq. (6) by the $\mp$ operator.

The periodicity of the chain now occurs between pairs, and r is now defined as the distance between cells. In an infinite chain, a cell would consist of a large mass and either of its neighboring, small masses. However, whenever the models are finite, the end conditions define a cell more strictly (see Fig. 4.)

There are, then, two vibrations for the two degrees of freedom per cell, one in which the two particles and, therefore, the center of mass move together, and one in which the two particles move in opposite directions such that the center of mass is stationary. The former is the acoustic vibration and the latter the optic. For the acoustic frequencies, the two masses vibrate with equal amplitude at low wavenumbers. As $k \rightarrow k_m$ the small masses become stationary so that the frequency of the highest acoustic mode is independent of the small mass. For the optic frequencies, the two masses vibrate with an amplitude ratio equal to the inverse of their mass ratio at low wavenumbers. As $k \rightarrow k_m$ the large mass becomes stationary so that the frequency of the highest optic mode is independent of the large mass. These four modes of vibration with the end restrictions are clearly observed on the ana-

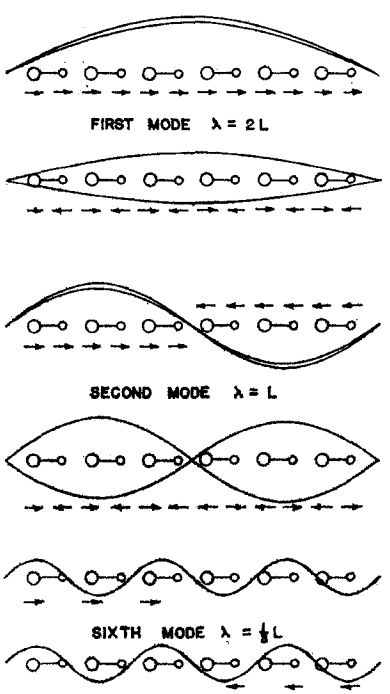

FIG. 4. Amplitude variation curves for 3 of the 6 modes for the 12-member, 6-cell diatomic chain.

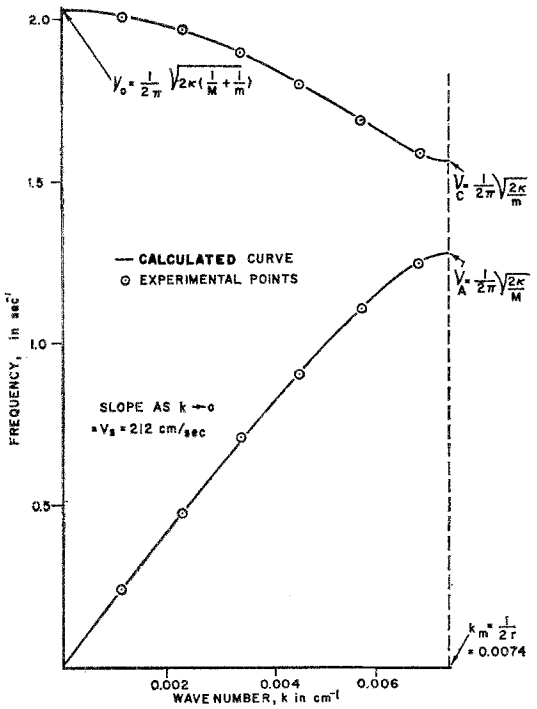

FIG. 5. The ν vs k diagram for a diatomic chain. The solid lines represent the calculated curves for the infinite chain and the points indicate the measured values for the 12-member, 6-cell chain.

log. Three of the six observed modes for the twelve-member, six-cell diatomic model are schematically shown in Fig. 4. As in the monatomic case, this figure shows the amplitudes and directions of vibration and the deviations from the above described modes due to the end effects.

The ν vs k diagram for the diatomic chain with constants, $\kappa=5040$ dyn/cm, $M=155.6$ g, $m=103.8$ g, and $r=68$ cm is shown in Fig. 5. The solid line is a plot of Eq. (6) for an infinite chain, and the points are measured values for the twelve-member chain. The latter exhibit excellent agreement and reveal the dispersion of the acoustic branch, the separation of the optic and acoustic branches, and the stopping or reflection band. The measured and calculated frequencies are shown in Table II.

A solid exhibiting such characteristics is known as a bandpass filter since it does not transmit waves with frequencies between ν_A and ν_C. For an infinite chain $\nu_A=(1/2\pi)(2\kappa/M)^{\frac{1}{2}}$ and $\nu_C=(1/2\pi)(2\kappa/m)^{\frac{1}{2}}$, from Eq. (6). Thus, for various diatomic chains, the width of the stopping band increases with increasing mass ratio. To demonstrate this point, the ν vs k diagrams for diatomic models with larger and smaller mass ratios were obtained and are shown in Fig. 6. These diagrams also demonstrate two points given mathematically above. It is seen that as the mass ratio becomes large, the acoustic branch approaches a sine curve while the optic branch becomes narrow and approaches a straight line. On the other hand, as the mass ratio approaches one, the width of the optic branch increases, the width of the stopping band approaches zero, and the dispersion of the acoustic branch decreases. When the ratio is precisely equal to one the frequency is no longer degenerate, and the periodicity reduces to the interparticle distances which doubles k_m. In this case, the ν vs k diagram is plotted as in Fig. 3.

From the ν vs k diagrams, the frequency spectra are derived. The frequency spectrum is merely the plot of the distribution of resonant frequencies of the solid, or model, with respect to the frequency. That is, $dk/d\nu$ is proportional to frequency distribution function $f(\nu)$. Plots of $dk/d\nu$ for the three examples in Fig. 6 were made graphically and are shown in Fig. 7. It is seen that the Debye approximation for the frequency spectrum,

$$f(\nu)d\nu=K\nu^2d\nu,$$

is very similar to the frequency spectrum ob-

TABLE II. Comparison of frequencies calculated from Eq. (6) and those experimentally measured for a 12-member, 6-cell diatomic model with the chain constants, $\kappa=5040$ dyn/cm, $M=155.6$ g, $m=103.8$ g, and $r=68$ cm.

Mode number	Wavenumber cm^{-1}	Calculated frequency cps	Measured frequency cps
1	1.13×10^{-3}	0.235	0.237
		2.011	2.01
2	2.26	0.474	0.474
		1.966	1.97
3	3.39	0.702	0.704
		1.899	1.90
4	4.52	0.912	0.916
		1.807	1.80
5	5.65	1.108	1.11
		1.694	1.69
6	6.78	1.255	1.26
		1.589	1.59

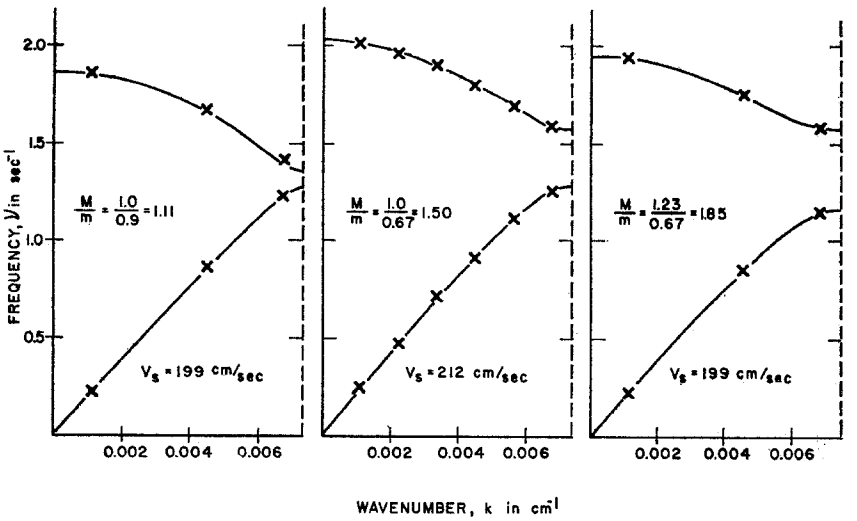

FIG. 6. Effect of varying the mass ratio in the diatomic chain on both the calculated and measured ν vs k diagram.

tained in the above manner for the monatomic model and the diatomic model as $M/m \rightarrow 1$.

The velocity of an elastic wave through a diatomic chain may also be obtained, as in the monatomic case, from the slope of the acoustic branch as $k \rightarrow 0$. For such a condition, the part of Eq. (6) in brackets approaches

$$(M+m)\{1-[4Mm/(M+m)^2]\alpha^2\}^{\frac{1}{2}},$$

which approximates

$$(M+m)\{1-[2Mm/(M+m)^2]\alpha^2\}.$$

Since $\alpha=\pi kr$, where r=distance between cells, the substitution of the above into Eq. (6) yields

$$\omega=\pi kr[2\kappa/(M+m)]^{\frac{1}{2}}.$$

Therefore,

$$V_s=\lim_{k\rightarrow 0}(\nu/k)=(r/2)[2\kappa/(M+m)]^{\frac{1}{2}}.$$

This velocity was measured as described above for the monatomic chain. For the above described diatomic model, the results were 212.0 cm/sec (chain constants), 212.4 cm/sec (experimental slope in Fig. 5), and 210 cm/sec (measured pulse velocity).

V. FURTHER APPLICATIONS IN LATTICE DYNAMICS

It is evident from the preceding sections that the linear-air-track analog of the one-dimensional chain successfully and quantitatively reproduces results which are well-known theorems in lattice dynamics. It should also be successful as a model to demonstrate unknown results in lattice dynamics, where mathematical methods are formidable. Several such topics are suggested as follows:

1. *Defects.* In order to understand the role of

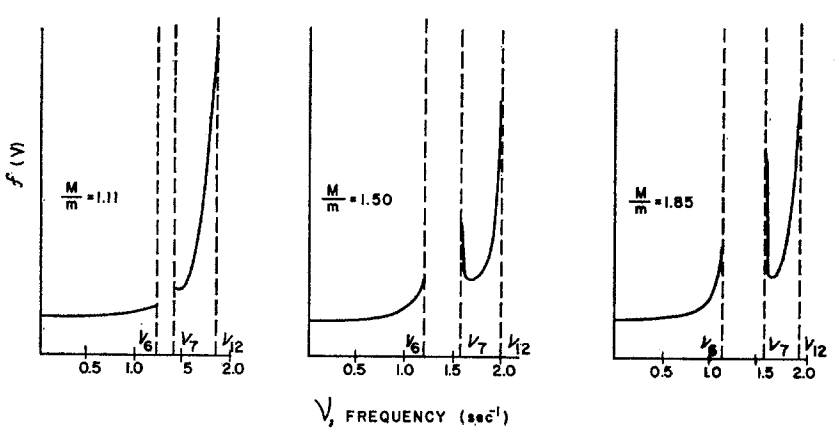

FIG. 7. The frequency spectra of the three diatomic chains represented in Fig. 6.

defects on the dispersion curves, several experiments were performed. In the 6-member monatomic chain, with cars of 155.6 g, fifty grams were added to one car. The effect was to lower slightly the observed frequencies as follows:

Mode No.	Perfect chain	One heavy defect
1	0.404 cps	0.385 cps
4	1.417	1.390
6	1.767	1.720

Second, when one of the cars was replaced by a light car (103.8 g), the frequencies were raised.

Mode No.	Perfect chain	One light defect
1	0.404 cps	0.420 cps
4	1.417	1.490
6	1.767	1.900

Third, in the diatomic 12-member chain, one heavy car was loaded with 50 extra grams. The results were that the optic branch was not shifted but that the acoustic branch was lowered. This agrees with the fact that at high wavenumbers, the optic frequencies are independent of the heavier sublattice.

Fourth, in the diatomic 12-member chain, one light car was loaded with 50 extra grams. In this case, the acoustic branch was not changed, but the optic branch was lowered at the high wavenumber end.

These results are plotted in Fig. 8. Further results on the nature of special defects are obviously possible with this model.

2. Harmonic and anharmonic behavior. In a harmonic solid, the frequency diagrams are not changed as the chain is compressed (lowering the interparticle distance). The model described here is found to behave harmonically. Anharmonic behavior could be investigated by the design and use of anharmonic springs between the cars. This would permit further research on the relationship between pure harmonic behavior and pure Hookian behavior.

3. Distant-neighbor interactions. The effect of distant neighbors could be studied by attaching

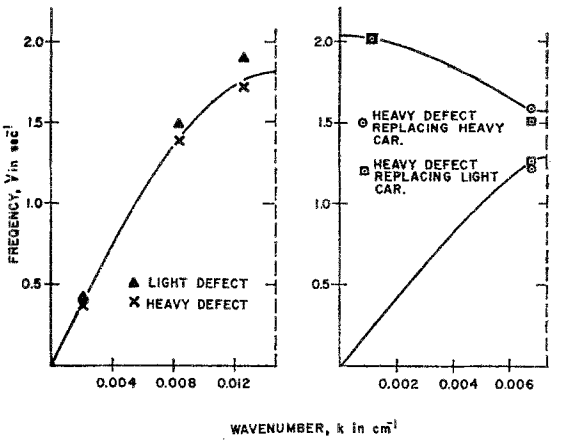

FIG. 8. Effect of various defects on the monatomic and diatomic models.

weak springs between alternate cars. This approach might clarify the point made by Brillouin[7] that the effect of distant neighbors is to make the wavenumber degenerate (that is, for each frequency, there may be more than one wavenumber in a branch).

4. Polyatomic chains. Systems of cars could be designed where a molecule (several cars) could be coupled together as a cell, and cells coupled as the cars are coupled in a monatomic chain. In this way, a multiple of acoustic and optic branches could be generated and examined.

5. Hindered rotation. On each car, a swivel could be mounted with a mass free to rotate about an axis perpendicular to the track. This gives rotational freedom as well as translational freedom, and thus the chain becomes a one-dimensional model of an organic crystal. Using this model, the relationship between Raman spectra and infrared spectra might be examined.

ACKNOWLEDGMENTS

The authors wish to thank J. D. Layfield for his contributions in the design and construction of the linear air track. Thanks are also due to the members of Physics 566, State University of New York, College of Ceramics at Alfred University.